Sub Topic: Reaction Kinetics

12th U.S. National Combustion Meeting
Organized by the Central States Section of the Combustion Institute
May 24–26, ~~2019~~ (Virtual) 2021
College Station, Texas

Extensive High-Accuracy Thermochemistry and Group Additivity Values for Automated Generation of Halocarbon Combustion Models

David Farina Jr.[1], Sai Krishna Sirumalla[1], and Richard H. West[1,]*

[1]*Department of Chemical Engineering, Northeastern University, Boston, MA 02115, USA*
[*]*Corresponding author:* r.west@northeastern.edu

Abstract: Standard enthalpies, entropies, and heat capacities are calculated for more than 14,000 halogenated species using a high-fidelity automated thermochemistry workflow. This workflow generates conformers at density functional tight binding (DFTB) level, optimizes geometries, calculates harmonic frequencies, and performs 1D hindered rotor scans at DFT level, and computes electronic energies at G4 level. The computed enthalpies of formation for 400 molecules show good agreement with literature references, but the majority of the calculated species have no reference in the literature. Thus, this work presents the most accurate thermochemistry for many halogenated hydrocarbons to date. This new dataset is used to train an extensive ensemble of group additivity values (GAV) and hydrogen bond increment groups (HBI) within the Reaction Mechanism Generator (RMG) framework. On average, the new group values estimate standard enthalpies for halogenated hydrocarbons within 3 kcal/mol of their G4 values. To demonstrate the significance of RMG's improved halogen thermochemistry, a model for $C_3H_2F_3Br$ (2-BTP) is generated, and flame speeds are compared to a literature mechanism. A significant contribution towards the automation of detailed modeling of halogenated hydrocarbon combustion, this research provides thermochemical data for thousands of novel halogenated species and presents a comprehensive set of halogen group additivity values.

***Keywords:* halocarbons, thermochemistry, flame suppression, automated mechanism generation**

1. Introduction

1.1 Halogenated Hydrocarbons (HHCs)

Halogenated hydrocarbons (HHCs) are commonly used as flame suppressants and refrigerant working fluids. The first generation of these compounds, chlorofluorocarbons (CFCs) and hydrochlorofluorocarbons (HCFCs), depleted the ozone layer and were banned worldwide under the Montreal Protocol in the 1980s [1]. The second generation, hydrofluorocarbons (HFCs), are ozone-friendly but are currently being phased out due to their high global warming potentials (GWPs) [2]. Despite these controls on high-GWP HFC production, a recent study discovered that emissions of HFC-23 (CHF_3), a potent greenhouse gas, reached an historic high in 2018 [3].

To address these environmental concerns, several low-GWP HHC refrigerants and suppressants have been proposed. However, the chemical properties that make these HFCs more environmentally friendly also increase their flammability [4]. Therefore, the combustion properties of these proposed HHCs are of the utmost concern. Since experimental studies of these properties are complex and costly, predictive kinetic modeling of HHC combustion is crucial in screening proposed compounds in order to facilitate their innovation and implementation.

Understanding the complex chemistry of new compounds and predicting their combustion behavior under different conditions requires the compilation and simulation of detailed kinetic mechanisms (or microkinetic models) which often contain thousands of elementary reactions and hundreds of intermediate species. Building these models by hand is extremely challenging and error-prone due to the vast number of possible species and reactions to consider, sparse thermokinetic data available in the scientific literature, and biases of the human choosing which pathways to pick. Thus, a tool that could generate these models automatically by enumerating and evaluating the many potential pathways by which HHCs combust would be instrumental in screening greener refrigerants and suppressants for flammability.

1.2 Reaction Mechanism Generator

Reaction Mechanism Generator (RMG) is an open-source software package that automatically builds detailed kinetic models by proposing elementary reactions and estimating chemical properties (physical, thermochemical, kinetic, solvation, etc.) using a database of reaction templates, thermokinetic data, and estimation methods [5]. These chemical properties are first sought in a database of known parameters, but are more commonly estimated using hierarchical decision trees. Thermochemical parameters ($\Delta_f H^{\ominus}_{298K}$, $S^{\ominus}_{298K}$, $Cp^{\ominus}_{300-2400K}$) are usually estimated using Benson's group additivity method [6] for closed-shell species and the Hydrogen Bond Increment (HBI) scheme [7] for radicals. RMG's group additivity values are derived from high fidelity experimental data supplemented with high level quantum chemistry data.

The success of RMG's rate-based algorithm in generating reliable kinetic models that capture all the essential chemistry in complex reacting systems depends heavily on the accuracy of thermokinetic parameters. As RMG was originally developed to study the kinetics of hydrocarbon combustion, its databases contain extensive, although not exhaustive, thermokinetic data for CHO chemistry. Since many short-lived intermediate species and elementary reactions are impossible to isolate and investigate experimentally, quantum chemistry methods are needed to calculate thermokinetic parameters. Recent progress on expanding RMG to model nitrogen [8], sulfur [9], and silicon [10] has shown that quantum chemistry calculations are a viable approach to expand RMG's databases and estimation methods to new chemical systems. Thus, adding high-accuracy halogen thermochemical data to RMG's thermodynamic libraries and group additivity trees is essential to extending RMG to model halocarbon combustion.

2. Methods/Experimental

2.1 The *enum-halocarb4* dataset

Due to a scarcity of thermochemical data for halogenated species in the literature, a new dataset, *enum-halocarb4*, was compiled as part of this work. In order to obtain high coverage and diversity of CHO-(F,Cl,Br) chemical space, this dataset was created by "halogenating" a systematically enumerated set of over 600 CHO species containing up to 4 heavy atoms generated by Margraf et al. [11]. This "halogenating" process involved systematic substitutions of halogen atoms (F,Cl,Br) for hydrogens using RDKit [12]. To obtain an initial set of halogenated species to calculate with the automated thermochemistry workflow, the set was pruned by removing cyclic species and radical species with more than one unpaired electron. The chemical composition of the 14,801 molecules in the *enum-halocarb4* is shown in Table 1.

Composition	Closed-Shell	Radical	Total
CHOF	1048	1591	2639
CHOCl	1040	1552	2592
CHOBr	721	721	1442
CHOFCl	852	923	1775
CHOFBr	1540	1858	3398
CHOClBr	932	1108	2040
CHOFClBr	447	468	915

Table 1: Composition of 14801 molecules in *enum-halocarb4*

2.2 Thermochemistry Workflow

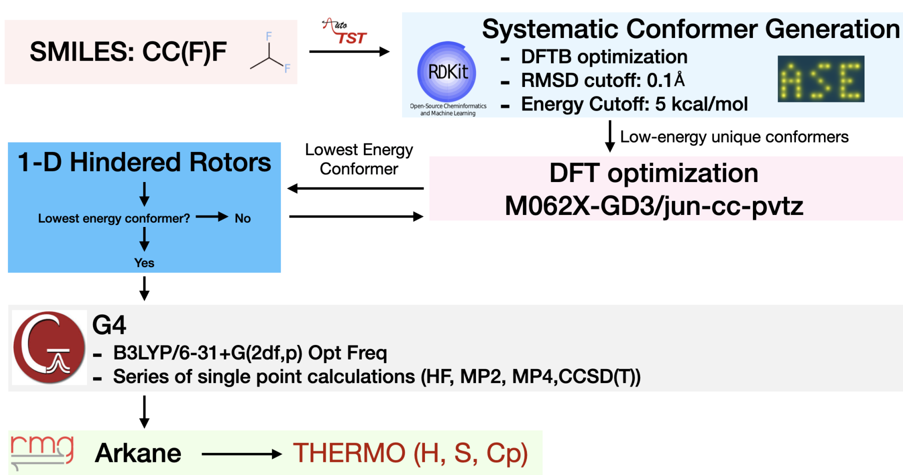

Figure 1: *ab-initio* Thermochemistry Workflow

The automated thermochemistry workflow used to calculate high-level thermochemical parameters (enthalpy, entropy, and heat capacity) of the *enum-halocarb4* dataset is shown in Figure 1. First, a SMILES representation of the molecule is used to generate a molecular graph of the species using RMG. Then, the molecule is embedded using RDKit [12] to create a 3D geometry. After embedding, conformers were investigated using the systematic conformer generation algorithm implemented in AutoTST [13]. This algorithm explores conformers by rotating dihedrals in 120° increments, varying cis/trans isomerism of double bonds, and alternating R/S sterochemistry for chiral centers. Conformers were optimized in ASE [14] using the dftb+ calculator [15] with the halorg-0-1 parameter set [16]. An ensemble of unique low-energy conformers was selected above a root-mean-square deviation of 0.1 Å and below an energy cutoff of 5 kcal/mol.

These conformers were re-optimized with DFT in Gaussian 16 [17] using M06-2X-D3/jun-cc-pvtz (the M06-2X functional with Grimme's D3 empirical dispersion [18] and the jun-cc-pvtz basis set [19]). Following all geometry optimizations, RMG's graph isomorphism algorithm was used to ensure that the optimized molecules matched the corresponding input SMILES. If the optimized conformer was not isomorphic with the input molecular graph, the conformer was discarded from the set. If all of the optimized conformers were not isomorphic, that molecule was deemed unstable and removed from *enum-halocarb4*.

After identifying the lowest energy conformer with M06-2X-D3/jun-cc-pvtz, 1D hindered rotors calculations were performed in Gaussian 16. For CHOF-containing molecules with internal rotors, the lowest energy conformer was optimized using B3LYP/6-31+G(2df,p) and rotor scans were performed in 10° increments with the same method. For molecules containing chlorine and bromine, the rotor scans were performed in 15° increments using M06-2X-D3/jun-cc-pvtz. If a lower energy conformer was found during the rotor scans, the conformer was reoptimized starting with the lower energy coordinates with DFT and the rotor scans were redone.

To obtain more accurate electronic energies, the lowest energy conformer was re-calculated with the Gaussian 4 (G4) compound method [20] in Gaussian 16. Lastly, to obtain thermochemistry in NASA polynomial form, the G4 energies and harmonic frequencies and the DFT rotor scans were passed to RMG's statistical mechanics calculator Arkane [21]. For species with internal rotors, Arkane's best fit algorithm was used to determine whether a cosine function or a Fourier series better fits the energy profile of the rotor scan.

2.3 Group Additivity Values

The thermochemical data calculated at G4 level in the *enum-halocarb4* dataset was used as training data to fit new halogen thermo groups in RMG. Three types of thermo additivity groups were derived: conventional Benson group additivity values (GAV), hydrogen bond increment groups (HBI) and non-next-nearest neighbor long-distance interaction groups. Figure 2 demonstrates how the three categories of groups combine to estimate the enthalpy of formation for a hydrofluorocarbon radical $C_4H_6F_3$ calculated in the *enum-halocarb4* dataset.

The new GAVs and HBIs were systematically created by generating every possible group with either a carbon or oxygen center atom, bonded to at least one halogen atom. To maintain RMG's performance for estimating CHO thermochemistry, existing groups were held fixed while new halogen groups were fit using scikit-learn's linear least square ridge regression method. 221 GAVs and 85 long distance halogen interaction groups were derived using thermochemical data ($\Delta_f H^{\ominus}_{298K}$, $S^{\ominus}_{298K}$, $Cp^{\ominus}_{300-2400K}$) for 6,578 closed-shell species in *enum-halocarb4* calculated using G4. Thermochemistry for 3,825 *enum-halocarb4* radicals were used to fit 76 halogen-containing HBI groups.

CCC(F)[C](F)F

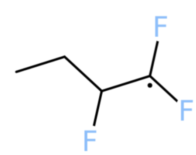

GAV	H298 (kcal/mol)
Cs-CsHHH:	-10.2
Cs-CsCsHH	-4.9
Cs-CsCsFH:	-55.2
Cs-CsFFH:	-107.4
Long-Distance	
Cs(F)2-Cs(F):	+4.7
HBI	
Csj-CsFF:	+100.5
H atom:	-52.1
Total =	-124.6
G4 =	-126.2
Error =	+1.6

Figure 2: Group additivity estimate of $C_4H_6F_3$ enthalpy

2.4 Reaction Mechanism Generation

To assess the ability of RMG's new halogen thermo groups to accurately estimate thermochemistry of intermediates created during automated generation of HHC combustion models, an RMG model was constructed for $C_3H_2F_3Br$ (2-BTP) and CF_3Br in methane flames. Before generating a model, a literature mechanism for 2-BTP from NIST [22] was imported into RMG. In order to teach RMG how these two suppressants behave in hydrocarbon flames, 727 of the 1,610 reactions in the literature mechanism were added as training reactions to RMG's reaction families. Then, an RMG model was built using the *Foundational Fuel Chemistry Model Version 1.0* [23] in RMG-database as a seed mechanism. The *enum-halocarb4* was used as an RMG thermo library during 2-BTP model generation, should RMG need thermochemistry for an intermediate in that dataset. The literature model contained 188 species and 1,610 reactions, whereas the RMG-built model contained 504 species and 9,515 reactions. For further validation (section 3.2) 122 of the 504 species in the RMG mechanism were recalculated at G4 level using the automated thermochemisty workflow previously discussed, and the calculated thermochemical properties were compared to group additivity estimates.

2.5 Flame Speed Simulations

The RMG 2-BTP model was compared to the literature mechanism by calculating 1D laminar flame speeds in Cantera [24]. The flame speeds were evaluated at 300K, 1 atm, and a wide range of methane/air equivalence ratios ($\phi = 0.5–1.2$) and suppressant volume fractions (0 – 0.05). Since there is a large discrepancy in the uninhibited methane burning velocity between the 2 models, the normalized flame speeds were compared by dividing the velocity of the suppressed flame by the velocity of the uninhibited flame.

3. Results and Discussion

3.1 Thermochemistry Workflow Benchmark

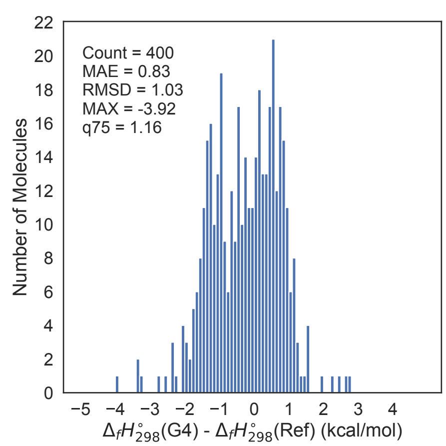

Figure 3: Enthalpies for halogenated species calculated at G4 level show good agreement with reference values

Figure 3 shows the distribution of the error for 400 molecules in the *enum-halocarb4* calculated at G4 level compared to reference enthalpies of formation from the Active Thermochemical Tables (ATcT) [25] and various literature sources [26–38]. With a mean absolute error (0.83 kcal/mol) within chemical accuracy ($\leq$ 1 kcal/mol) for the benchmark set, G4 is a suitable, relatively low cost composite quantum chemistry method for high-fidelity and high-throughput calculations of HHCs. However, for heavily halogenated systems, G4 and other composite methods do not compute enthalpies within chemical accuracy [39]. Calculated G4 enthalpies for C_2Cl_5 and C_2Cl_6 in *enum-halocarb4* are more than 3 kcal/mol lower than ATcT values. Therefore, heavily halogenated molecules in the *enum-halocarb4* likely have higher errors than their more sparsely halogenated counterparts.

3.2 Group Additvity Value Predictions

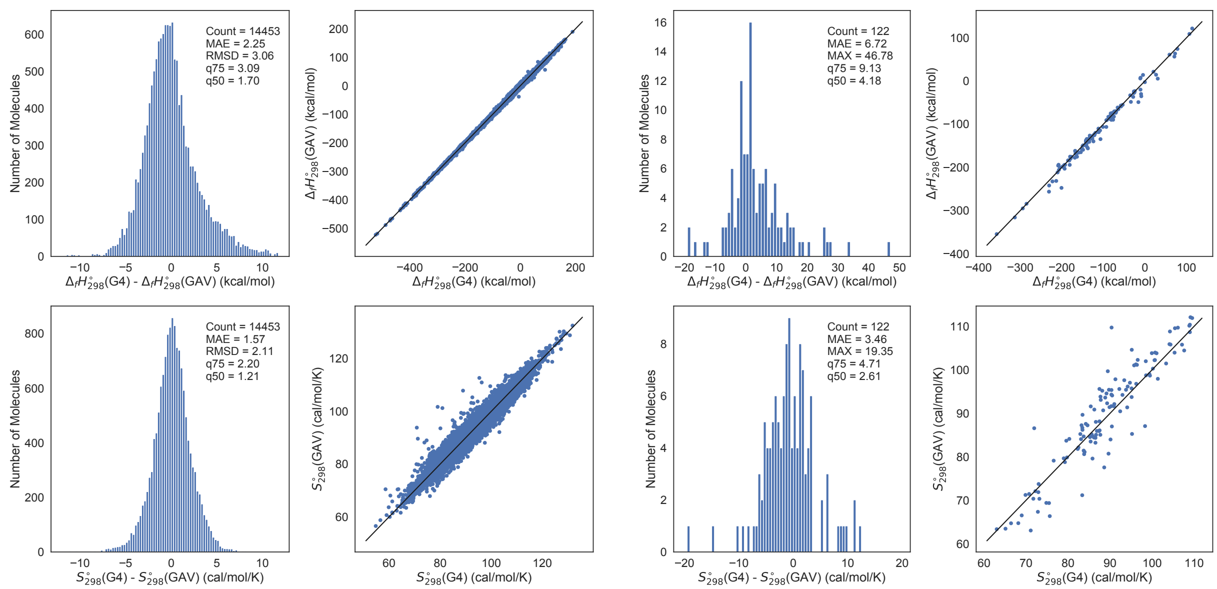

(a) *enum-halocarb4*

(b) RMG 2-BTP

Figure 4: Group additivity estimated enthalpies and entropies for halogenated species in *enum-halocarb4* and RMG 2-BTP model

The performance of the thermo groups derived in this work at estimating standard enthalpies and entropies for 14,453 species in the *enum-halocarb4* is shown in Figure 4a. On average, the halogen GAVs estimate enthalpies of formation within 3 kcal/mol of the G4 calculations. This is on par with RMG's CHO thermo GAVs which typically estimate enthalpies within 2-3 kcal/mol. Based on the halogen GAV performance on the large *enum-halocarb4* dataset, RMG's new halogen GAVs appear to be reliable at accurately predicting thermochemical properties for a wide range of HHCs.

Figure 4b shows the predictive capability of the halogen GAVs for 122 species in the RMG 2-BTP model. With a mean absolute error of 6.7 kcal/mol, the GAVs were significantly less accurate at estimating enthalpies for 2-BTP intermediates than for the *enum-halocarb4* training set. The poorer performance is largely due to the presence of cyclic species and biradicals in the 2-BTP model since there are no biradicals or cyclic molecules in *enum-halocarb4*. When cyclic species and biradicals are removed, the mean absolute error is reduced to 4.7 kcal/mol.

3.3 Flame Speeds

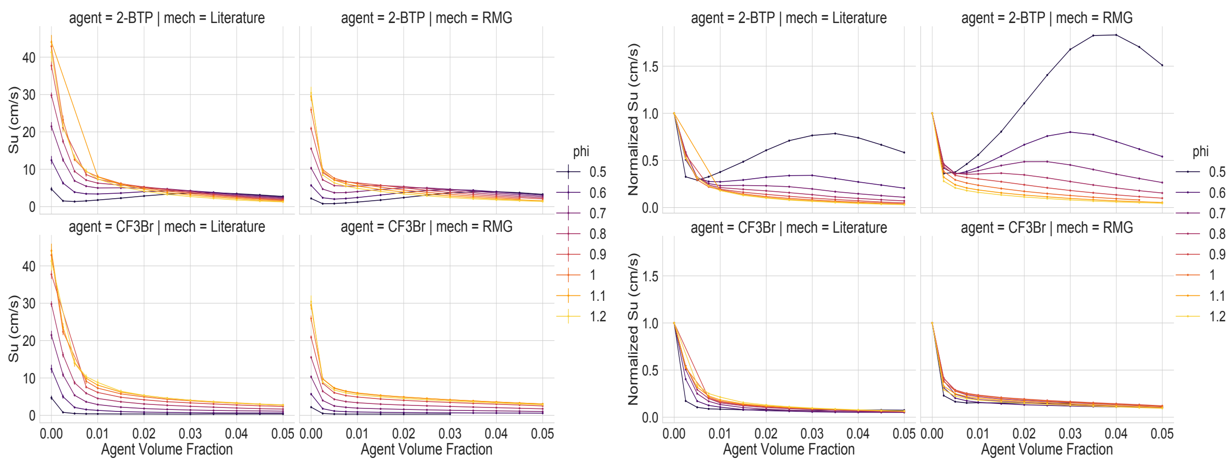

(a) Flame Speeds

(b) Normalized Flame Speeds

Figure 5: Computed burning velocities of methane flames for RMG and literature mechanisms with added suppressants 2-BTP or CF_3Br.

Figure 5 shows how the premixed methane/air laminar flame speeds change for the literature and RMG mechanisms when the suppressing agent (2-BTP or CF_3Br) is added. Although there is a large disagreement in the uninhibited methane burning velocities for the two models, the RMG model shows remarkably good agreement with the literature mechanism over a wide range of equivalence ratios and suppressant volume fractions. Importantly, RMG is able to automatically "discover" the important bromine flame inhibition reactions that scavenge H atoms and suppress flame propagation. Additionally, the RMG model is able to capture the "fuel effect" of 2-BTP, discussed in [40], which enhances flame speeds for lean methane/air flames.

4. Conclusions

This research provides thermochemical data for thousands of novel halogenated species and presents a comprehensive set of halogen group additivity values. The halogen GAVs accurately estimate enthalpies of formation for acylcic closed-shell and radical species in *enum-halocarb4* but show poorer performance for rings and biradicals for which more thermochemical training data are needed. The new halogen GAVs and *enum-halocarb4* thermochemistry data were implemented in RMG and used to automatically construct a 2-BTP kinetic model with 504 species and 9,515 reactions. Predicted methane/air flame speeds with added suppressant were in close agreement for the literature and RMG 2-BTP mechanisms, even though the RMG model has 316 more species and 7,905 more reactions. Thus, although flame speeds appear to be insensitive to these newly discovered species and reactions, a more thorough investigation into RMG's mechanism is necessary to determine if these intermediates and pathways are important to halocarbon flame suppression.

5. Acknowledgements

This material is based upon work supported by the National Science Foundation under Grant No. 1751720. The authors acknowledge Information Technology Services, Research Computing at Northeastern University for providing high performance computing and storage, related software, visualization, and consulting resources.

References

[1] Montreal Protocol on Substances that Deplete the Ozone Layer Final Act 1987, Journal of Environmental Law 1 (1989) 128–136. DOI: 10.1093/jel/1.1.128.

[2] K. Harby, Hydrocarbons and their mixtures as alternatives to environmental unfriendly halogenated refrigerants: An updated overview, Renewable and Sustainable Energy Reviews 73 (2017) 1247–1264. DOI: 10.1016/j.rser.2017.02.039.

[3] K. M. Stanley, D. Say, J. Mühle, C. M. Harth, P. B. Krummel, D. Young, S. J. O'Doherty, P. K. Salameh, P. G. Simmonds, R. F. Weiss, R. G. Prinn, P. J. Fraser, and M. Rigby, Increase in global emissions of HFC-23 despite near-total expected reductions, Nature Communications 11 (2020) 397. DOI: 10.1038/s41467-019-13899-4.

[4] G. Linteris and V. Babushok, Numerically-Predicted Velocities of C 1 and C 2 Hydrofluorocarbon Refrigerant Flames with Air Engineering Laboratory , National Institute of Standards and Technology * Corresponding Author, (2018) 1–10.

[5] C. W. Gao, J. W. Allen, W. H. Green, and R. H. West, Reaction Mechanism Generator: Automatic construction of chemical kinetic mechanisms, Comput. Phys. Commun. 203 (2016) 212–225. DOI: 10.1016/j.cpc.2016.02.013.

[6] S. W. Benson, F. R. Cruickshank, D. M. Golden, G. R. Haugen, H. E. O'Neal, A. S. Rodgers, R. Shaw, and R. Walsh, Additivity rules for the estimation of thermochemical properties, Chemical Reviews 69 (1969) 279–324. DOI: 10.1021/cr60259a002.

[7] T. H. Lay, J. W. Bozzelli, A. M. Dean, and E. R. Ritter, Hydrogen Atom Bond Increments for Calculation of Thermodynamic Properties of Hydrocarbon Radical Species, J. Phys. Chem. 99 (1995) 14514–14527. DOI: 10.1021/j100039a045.

[8] A. G. Dana, B. Buesser, S. S. Merchant, and W. H. Green, Automated Reaction Mechanism Generation Including Nitrogen as a Heteroatom, Int Chem Kinet 50 (2018) 243–258. DOI: 10.1002/kin.21154.

[9] C. A. Class, A. K. Vasiliou, Y. Kida, M. T. Timko, and W. H. Green, Detailed kinetic model for hexyl sulfide pyrolysis and its desulfurization by supercritical water, Phys. Chem. Chem. Phys. 21 (2019) 10311–10324. DOI: 10.1039/C9CP00234K.

[10] B. L. Slakman, H. Simka, H. Reddy, and R. H. West, Extending Reaction Mechanism Generator to Silicon Hydride Chemistry, Ind & Eng Chem Res 55 (2016) 12507–12515. DOI: 10.1021/acs.iecr.6b02402.

[11] J. T. Margraf and K. Reuter, Systematic Enumeration of Elementary Reaction Steps in Surface Catalysis, ACS Omega 4 (2019) 3370–3379. DOI: 10.1021/acsomega.8b03200.

[12] G. Landrum, *RDKit: Open-source cheminformatics*, URL: http://www.rdkit.org.

[13] P. Bhoorasingh, B. Slakman, F. S. Khanshan, J. Cain, and R. West, Kinetic data for manuscript describing the AutoTST algorithm for automated Transition State Theory calculations of chemical reaction rates. figshare.com (2016), DOI: 10.6084/m9.figshare.4234160.v1.

[14] A. H. Larsen et al., The atomic simulation environment—a Python library for working with atoms, Journal of Physics: Condensed Matter 29 (2017) 273002. DOI: 10.1088/1361-648X/aa680e.

[15] B. Aradi and B. Hourahine, *dftbplus/dftbplus [DFTB+]: Release 17.1*, English, 2017, DOI: 10.5281/zenodo.809965.

[16] T. Kubař, Z. Bodrog, M. Gaus, C. Köhler, B. Aradi, T. Frauenheim, and M. Elstner, Parametrization of the SCC-DFTB method for halogens, J. Chem. Theory Comput 9 (2013) 2939–2949. DOI: 10.1021/ct4001922.

[17] M. J. Frisch et al., *Gaussian 16 Revision B.01*, Gaussian Inc. Wallingford CT, 2016.

[18] S. Grimme, J. Antony, S. Ehrlich, and H. Krieg, A consistent and accurate ab initio parametrization of density functional dispersion correction (DFT-D) for the 94 elements H-Pu, Chem Phys 132 (2010), DOI: 10.1063/1.3382344.

[19] E. Papajak, J. Zheng, X. Xu, H. R. Leverentz, and D. G. Truhlar, Perspectives on basis sets beautiful: Seasonal plantings of diffuse basis functions, Journal of Chemical Theory and Computation 7 (2011) 3027–3034. DOI: 10.1021/ct200106a.

[20] L. A. Curtiss, P. C. Redfern, and K. Raghavachari, Gaussian-4 theory, Chem Phys 126 (2007), DOI: 10.1063/1.2436888.

[21] *Arkane: Automated Reaction Kinetics and Network Exploration*, Accessed: 2019–01-29, URL: https://reactionmechanismgenerator.github.io/RMG-Py/users/arkane/.

[22] D. R. Burgess, V. I. Babushok, G. T. Linteris, and J. A. Manion, A Chemical Kinetic Mechanism for 2-Bromo-3,3,3-trifluoropropene (2-BTP) Flame Inhibition, Int Chem Kinet 47 (2015) 533–563. DOI: 10.1002/kin.20923.

[23] Y. T. G. P. Smith and H. Wang, *Foundational Fuel Chemistry Model Version 1.0*, 2016, URL: http://nanoenergy.stanford.edu/ffcm1.

[24] D. G. Goodwin, H. K. Moffat, and R. L. Speth, *Cantera: An Object-oriented Software Toolkit for Chemical Kinetics, Thermodynamics, and Transport Processes*, http://www.cantera.org, Version 2.3.0, 2017, DOI: 10.5281/zenodo.170284.

[25] *Active Thermochemical Tables: version 1.122p*, URL: https://atct.anl.gov/Thermochemical%20Data/version%201.122p/.

[26] K. R. Jorgensen and M. Cadena, Theoretical study of bromine halocarbons: Accurate enthalpies of formation, Comp and Theo Chem 1141 (2018) 66–73. DOI: 10.1016/j.comptc.2018.08.016.

[27] E. Paulechka and A. Kazakov, Critical Evaluation of the Enthalpies of Formation for Fluorinated Compounds Using Experimental Data and High-Level Ab Initio Calculations, Chem Eng Data 64 (2019) 4863–4874. DOI: 10.1021/acs.jced.9b00386.

[28] N. L. Haworth, M. H. Smith, G. B. Bacskay, and J. C. Mackie, Heats of formation of hydrofluorocarbons obtained by Gaussian-3 and related quantum chemical computations, Phys Chem A 104 (2000) 7600–7611. DOI: 10.1021/jp000475c.

[29] D. L. Purnell and J. W. Bozzelli, Thermochemical Properties: Enthalpy, Entropy, and Heat Capacity of C2-C3 Fluorinated Aldehydes. Radicals and Fluorocarbon Group Additivity, Phys Chem A 123 (2019) 650–665. DOI: 10.1021/acs.jpca.8b09065.

[30] H. Wang, Á. Castillo, and J. W. Bozzelli, Thermochemical Properties Enthalpy, Entropy, and Heat Capacity of C1-C4 Fluorinated Hydrocarbons: Fluorocarbon Group Additivity, Phys Chem A 119 (2015) 8202–8215. DOI: 10.1021/acs.jpca.5b03912.

[31] J. M. Hudzik, L. R. Stoler, J. W. Bozzelli, and J. F. Liebman, Thermochemistry of Fluorinated Dimethyl and Ethyl Methyl Ethers and Corresponding Radical Species, Chem Eng Data 65 (2020) 1594–1616. DOI: 10.1021/acs.jced.9b01034.

[32] Á. Ganyecz, M. Kállay, and J. Csontos, Accurate Theoretical Thermochemistry for Fluoroethyl Radicals, Phys Chem A 121 (2017) 1153–1162. DOI: 10.1021/acs.jpca.6b12404.

[33] Á. Ganyecz, M. Kállay, and J. Csontos, High Accuracy Quantum Chemical and Thermochemical Network Data for the Heats of Formation of Fluorinated and Chlorinated Methanes and Ethanes, Phys Chem A (2018) acs.jpca.8b00614. DOI: 10.1021/acs.jpca.8b00614.

[34] J. J. Csontos, Z. Z. Rolik, S. Das, M. Kállay, and M. Kállay, High-Accuracy Thermochemistry of Atmospherically Important Fluorinated and Chlorinated Methane Derivatives, Phys Chem A 114 (2010) 13093–13103. DOI: 10.1021/jp105268m.

[35] S. Snitsiriwat, S. Yommee, and J. W. Bozzelli, Thermochemistry of Intermediates and Products in the Oxidation Reaction of 1,1,2-Trifluoroethene via OH Radical, Phys Chem A 123 (2019) 8017–8027. DOI: 10.1021/acs.jpca.9b06647.

[36] H. Wang and J. W. Bozzelli, Thermochemical Properties and Bond Dissociation Energies for Fluorinated Methanol, CH3-xFxOH, and Fluorinated Methyl Hydroperoxides, CH3-xFxOOH: Group Additivity, Phys Chem A 120 (2016) 6998–7010. DOI: 10.1021/acs.jpca.6b05293.

[37] H. Y. Sun and J. W. Bozzelli, Structures, rotational barriers, and thermochemical properties of beta-chlorinated ethyl hydroperoxides, Phys Chem A 107 (2003) 1018–1024. DOI: Doi10.1021/Jp022298g.

[38] A. Karton, S. Parthiban, and J. M. Martin, Post-CCSD(T) ab initio thermochemistry of halogen oxides and related hydrides xox, xoox, hox, xo, and hxo, (x = f, cl), and evaluation of dft methods for these systems, Phys Chem A 113 (2009) 4802–4816. DOI: 10.1021/jp8087435.

[39] A. Karton, N. Sylvetsky, and J. M. Martin, W4-17: A diverse and high-confidence dataset of atomization energies for benchmarking high-level electronic structure methods, Journal of Computational Chemistry 38 (2017) 2063–2075. DOI: 10.1002/jcc.24854.

[40] V. I. Babushok, G. T. Linteris, D. R. Burgess, and P. T. Baker, Hydrocarbon flame inhibition by C3H2F3Br (2-BTP), Combustion and Flame 162 (2015) 1104–1112. DOI: 10.1016/j.combustflame.2014.10.002.